Noise–mediated self–organization in mutually shading sunflowers

Chantal Nguyen*[a], Imri Dromi*[b], Aharon Kempinski[b], Gabriella E. C. Gall[b,c,d], Orit Peleg†[a,e,f], Yasmine Meroz‡[b]

[a] *BioFrontiers Institute, University of Colorado, Boulder, CO, USA*
[b] *School of Plant Science and Food Security, Tel Aviv University, Tel Aviv, Israel*
[c] *Zukunftskolleg, Department of Biology, University of Konstanz, Konstanz, Germany*
[d] *Centre for the Advanced Study of Collective Behaviour, Konstanz, Germany*
[e] *Department of Computer Science, University of Colorado, Boulder, CO, USA*
[f] *Santa Fe Institute, Santa Fe, NM, USA*

Abstract

Examples of collective behavior in biological systems are widespread; however, less attention has been given to plant systems. This is mostly due to the conceptually different type of movements in plants, classified as tropic, growing in the direction of external stimuli; or nastic, inherent movements due to internal cues such as the exploratory circumnutations. Here we study a system of mutually shading neighboring sunflowers, where interactions mediated by the shade response have been found to underpin a self-organized zig-zag growth pattern. We develop a minimal model which describes interacting sunflowers as growing repulsive disks tethered to an initial position, and interprets circumnutations as noise. Informing our model with experimental values enables us to identify the role of circumnutations as facilitating the observed self-organization.

Keywords: plant tropism, shade avoidance, collective behavior, self-organization, sunflowers, minimal model

*These authors have contributed equally to this work.
†orit.peleg@colorado.edu
‡jazz@tauex.tau.ac.il

Introduction

Self-organized systems are widespread in biological systems, where local interactions between components of the system lead to the emergence of order, often initiated by random fluctuations amplified by positive feedback [1, 2, 3, 4, 5]. Examples are ubiquitous, ranging from the molecular to the ecosystem scale [5], generally involving either pattern formation, driven by competition and resource availability, or collective behavior of social organisms, driven by communication and transfer of information [6, 7, 8, 9, 10].

However, less attention has been given to plant systems, where few observations have been reported, mostly concerning pattern formation, for example, in vegetation [11, 12, 13], and even less focus on dynamical systems driven by communication between individuals. This is in part due to the fact that movement in plants is generally driven by growth, which is too slow for us to perceive, and therefore not associated with a dynamical system. Furthermore, the mathematical description of dynamics of sessile growing systems is conceptually different form motile systems, accounting for elongation and the addition of material.

Here we focus on the experimental observation of the spatial self-organization of sunflower crops growing in a 1D row at high densities, as initially reported by Pereira et al. [14]. This was shown to be mediated by the shade avoidance response of neighboring plants, where plant organs grow away from the shade caused by neighbors [15] and toward blue light available in horizontal gaps in the canopy, ultimately enhancing light interception [16, 17, 18]. This type of directional response is called a tropism, the kinematics of which are mathematically well described [19, 20].

The observed self-organization was found to be triggered by a few pioneer plants who become shaded by neighbors and who orient their shoot toward the least shaded side of the row. The immediate neighbors bend in response to the resulting R/FR gradient and, in turn, generate a R/FR gradient in the opposite direction for the next neighbor in the row, thus propagating a sensory signal manifested by a wave of alternating inclinations of neighboring plants, and resulting in a final zig-zag conformation providing a more favorable light environment [14]. Self-organization is generally facilitated by noise, which in this system is manifested by plant cirumnutations, which are inherent periodic growth-driven movements (termed nastic movements). While circumnutations are beneficial, enabling the system to explore possible configurations in order to reach an optimum, they also pose a cost to the plant, both due to the

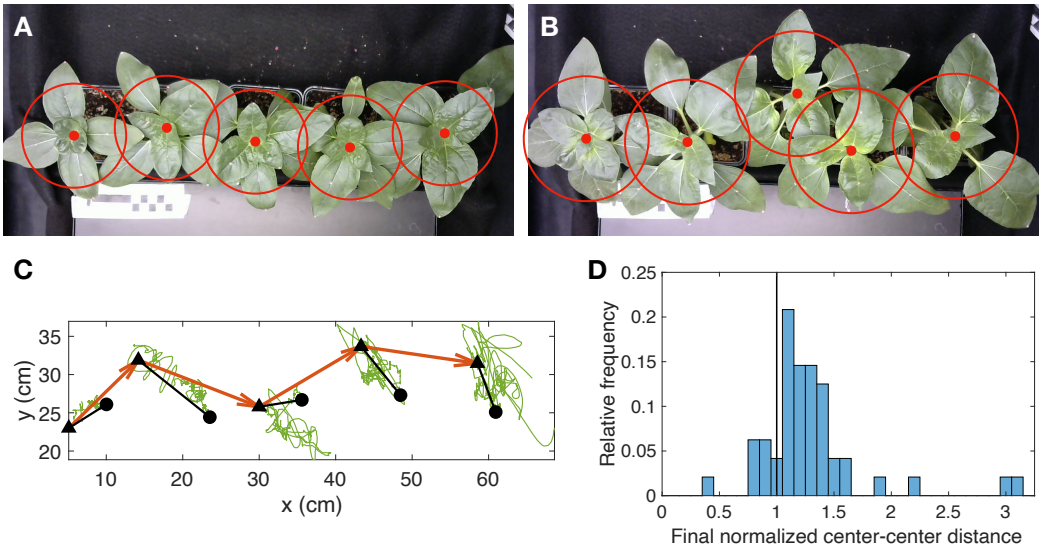

Figure 1: Plants grown in a dense row deflect away from each other to minimize their mutual shading. A: Plants are arranged in a dense horizontal row on the first day of recording. Red dots indicate manually-annotated center points. Red circles illustrate the model representation of crowns as circles in the x-y plane. B: By three days, plants deflect above and below the abscissa. C: Example trajectories (green lines) of crown centers from an 8-day recording. Black dots indicate initial positions of crown centers; black triangles indicate final positions. Orange arrows illustrate the center-center separation between pairs of adjacent plants. D: Histogram of the final center-center separation between pairs of adjacent plants, from 12 multiple-plant experiments. The separation values are normalized by the center-center separation in the initial frame. Values to the right of the black line indicate a final separation greater than that of the initial separation.

continuous change in leaf orientation (which, by definition, will not be in the direction of light for part of the time), as well as due to the mechanical cost of drooping sideways compared to growing straight.

Here, we study the self-organization dynamics of this system by developing a minimal model which enables us to shed light on the interplay between the mutual shading interactions and circumnutations, or noise. Informing our model with experimental data, we find that circumnutations are such that they maximize the light exposure of the collective, while minimizing the associating cost.

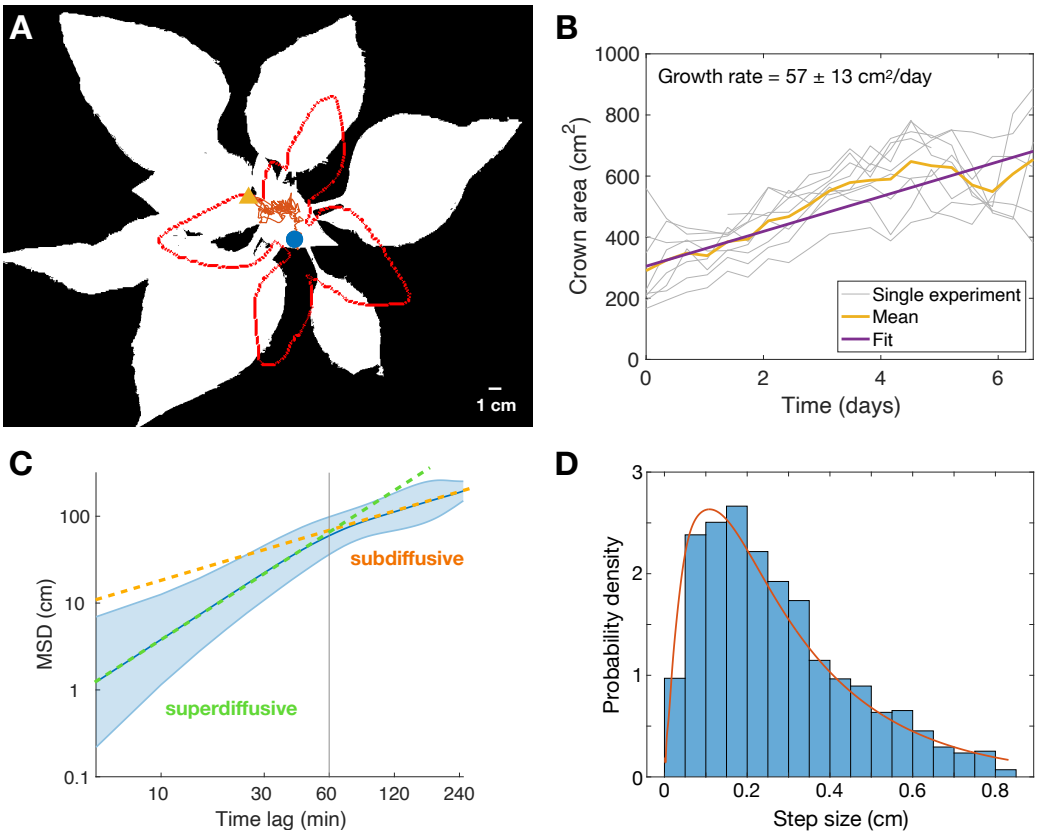

Figure 2: Characterization of single-plant growth and nastic movements. A: Image segmentation of plant crowns. The outline of the plant crown at the start of the recording is indicated by a red line, with the centroid marked by a blue dot. The white region represents the segmented plant crown after 10 days, with the corresponding centroid marked by a yellow triangle. The orange line illustrates the trajectory of the centroid over the course of the recording. B: Extracting the growth rate of the crown. Gray curves indicate the area of the crown as a function of time for individual single-plant experiments. The orange curve indicates the mean across experiments. The data from each experiment is individually fit to a line, and the mean of the slopes from each of the linear fits represents the growth rate of the crown (57 ± 13 cm^2/day). The violet line represents the average of the linear fits. C: The mean squared displacement for a single plant trajectory demonstrates a superdiffusive regime for time lag < 60 min, with an exponent of approximately 1.6, and a subdiffusive regime for time lag > 60 min, with an exponent of approximately 0.8. D: Step size distribution: histogram of distances between centroids measured in pairs of frames 1 hour apart (blue bars) and corresponding kernel density estimate (red line), with a mean of 0.29 cm.

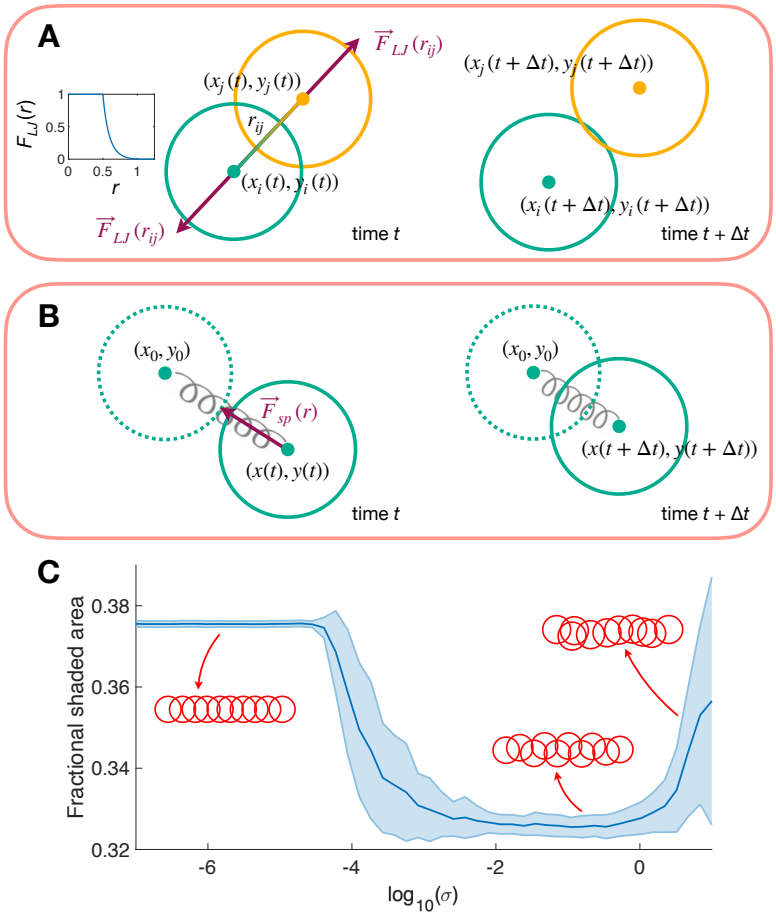

Figure 3: Self-organization emerges from minimal model describing interplay between repulsion and noise. A: Two overlapping crowns experience repulsion described by a modified Lennard-Jones force ($\vec{F}^{\,i}_{LJ}(\vec{r}^{\,ij})$). At time t, the two crowns are separated by a distance r_{ij} which is less than the sum of their radii. At time $t + \Delta t$, the plants deflect in opposite directions to reduce the shaded area. B: A crown is tethered to a point (x_0, y_0) by a spring. When a crown is displaced from the tether point by a distance r, it experiences a restoring spring force ($\vec{F}_{sp}(r)$). C: The mutual shaded area in a plant system decreases as a function of the noise (σ, the variance of the components of the noise term $\vec{\xi}$) in individual plant movements, reaching a minimum where symmetry breaking results in the plants self-organizing into an alternately-deflecting "zig-zag" pattern. For high noise, random movements dominate over repulsive interactions, producing disordered configurations that can result in greater shaded area. For very low noise, plants remain close to their tethering points due to the lack of symmetry-breaking fluctuations that push plants off the horizontal axis.

Materials and Methods

Plant growth conditions

We used sunflower seeds of the 'EMEK 6' variety (Sha'ar Ha'amakim Seeds). The seeds were first cooled in a refrigerator (seed stratification) at 5°C, peeled from their shell coats, and soaked in water for 24 hours. Each seed was then placed in a plastic test tube filled with wet Vermiculite and left to germinate in a growth chamber at 24°C, with a relative humidity of 72% and a 12:12 h light:dark photoperiod. The light intensity in the chamber was 22.05 W/m^2. Germination occurred after 4-7 days for each batch. Following germination, 3- to 7-cm-tall seedlings with two to four leaves that appeared healthy and well-separated were transplanted in 10 cm $\times$ 10 cm-wide and 15 cm-tall black plastic pots containing garden soil. The plants were exposed to white LED light with intensity 41.92 W/m^2 on a 16:8 h light:dark cycle, and the setup was enclosed with black fabric to eliminate sources of reflection. The ambient temperature was approximately 26°C during the light period and 28°C during the dark period, and the humidity ranged between 43-51%. Each plant was watered with 100 mL of a 0.2% 20-20-20 NPK fertilizer solution every 2 days. Plants were maintained in this setup for approximately one week.

Image acquisition

Plants were then selected for single-plant or multiple-plant assays that took place in conditions similar to the growth conditions described above, with the exception of light intensity at 27.05 W/m^2. In single-plant assays, plants were maintained in the enclosed experimental setup for 7-10 consecutive days. Multiple-plant assays consisted of five plants in individual pots closely arranged side-by-side in a horizontal row, again for 7-10 consecutive days (Fig. 1A-B).

Each plant assay was recorded from a top-down view with a Logitech C270 HD webcam. Images were acquired every 5 minutes during the light period using a Raspberry Pi Model 4 single-board computer.

We perform image segmentation and centroid tracking on videos of plants grown in individual setups using the colorThresholder function in MATLAB (MathWorks Inc., Natick, MA), from which we determine the area of the plant crown in top-down views. For videos of plants grown in multiple-plant setups, plant crowns can overlap from the top-down views, complicating image segmentation; instead of tracking the centroid of each connected component,

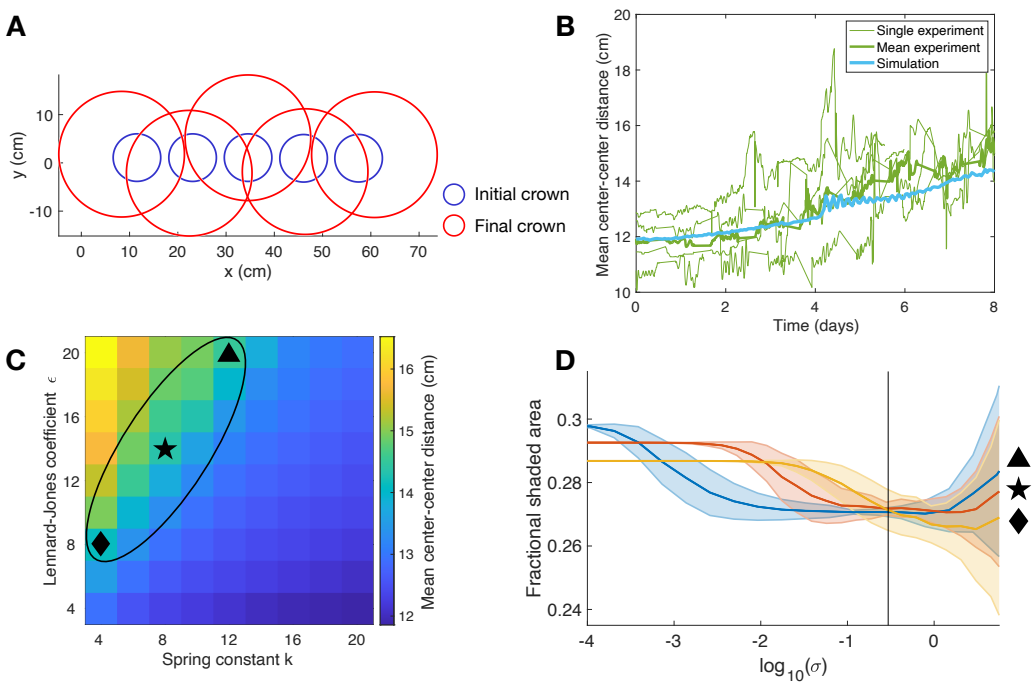

Figure 4: A: Initial (blue circles) and final (red circles) configurations of plant crowns over 8 simulated days. B: The center-center distance between pairs of adjacent crowns increases over time (single experiments shown as thin green lines, while the mean over experiments is shown as a thick green line). The blue line shows the center-center distance over the course of a simulation with growth rate 57 cm^2/day and variance of fluctuations $\sigma = 0.29$. C: Final center-center separation varies as a function of the spring constant k and Lennard-Jones coefficient ϵ. Oval represents a regime where the center-center separation is near that of experimental values shown in panel B. D: Fractional shaded area as a function of noise (σ) for the three pairs of ϵ and k values marked by a diamond, star, and triangle in panel C. Black vertical line indicates the experimentally-determined value of $\sigma = 0.29$ cm, which lies in the trough of each of the curves.

we manually annotate the center point of each crown in the first frame of the video and track its position using the DLTdv tracking software [21].

Extracting growth and behavioral parameters from experimental data

In multiple-plant assays, we observe that the crowns of plants originally arranged in dense horizontal rows (Fig. 1A) will expand and deflect off the original horizontal axis to avoid mutual shade (Fig. 1B). Example trajectories of the tracked crown centers over the course of a multiple-plant experiment are shown in Fig. (1C); at the end of each experiment, we determine the

mean separation between the crown centers of pairs of neighboring plants. We observe that for most plant pairs across 12 experiments, the final center-center distance is greater than the initial distance (Fig. 1D), indicating that crowns deflect away from one another in dense growth setups.

These observations of multiple-plant experiments motivate our development of a model that describes how repulsion between shading plants, and noisy individual plant movements, can lead to emergent self-organized patterns of alternately-deflecting plant crowns. From single-plant assays, we quantify the growth rate of a plant crown and its movement over time, in order to fit parameters of this model, as described in later sections.

From each of 8 recordings of single-plant experiments, we segment the plant crown (Fig. 2A) and compute a linear fit to the area of the crowns as a function of time (Fig. 2B). We average the slopes of the fitted lines to obtain a crown growth rate of 57 ± 13 cm^2/day.

We determine the mean squared displacement (MSD) of the centroid of the segmented plant crown (Fig. 2C). As a single plant recording consists of 16 hours of consecutive footage per day at a rate of one frame every five minutes, for a total of up to 10 consecutive days, we partition the resulting centroid trajectory into individual days and compute the MSD for each day. The average over the daily MSD is shown in Fig. 2C. The MSD reveals superdiffusive motion over shorter (< 60 min) timescales and subdiffusion over longer (≥ 60 min) timescales. We interpret this as representing a bounded diffusion of the crown, which later motivates our inclusion of a tethering spring force in the model that prevents crowns from deflecting infinitely far from their initial positions over time.

We represent circumnutations of the plant as random noise, where the variance of the noise represents the magnitude of the plant's nastic movements. To estimate this magnitude, we determine the "step size" distribution of the magnitude of displacements across pairs of frames separated by 1 hour (Fig. 2D). We then model the fluctuations in plant position as normally distributed with a variance equal to the mean of the step size distribution (0.29 cm).

Results

Minimal model of shade avoidance response

We formulate a model of crown deflections in the 2-D plane by modeling each plant as a circular crown with an area that grows linearly in time. When the separation between a pair of crowns is less than the sum of their radii,

each crown experiences a repulsive modified Lennard-Jones force of equal magnitude (Fig. 3A). The crown is tethered to its initial x-y position (x_0, y_0) by a spring, such that a deflection of the crown from its tether point induces a restoring spring force (Fig. 3B).

The spring force $\vec{F}^{\,i}_{sp}$ (Fig. 3B) on crown i is given by

$$\vec{F}^{\,i}_{sp} = -k(\vec{r}^{\,i} - \vec{r}^{\,i}_0), \tag{1}$$

where k is the spring constant, $\vec{r}^{\,i}$ denotes the position vector of the center of crown i, and $\vec{r}^{\,i}_0$ is the position vector of the tethering point of crown i.

For a system consisting of two crowns i and j with respective radii ρ^i and ρ^j and separated by the vector $\vec{r}^{\,ij} = \vec{r}^{\,j} - \vec{r}^{\,i}$, the modified Lennard-Jones force $\vec{F}^{\,i}_{LJ}$ (Fig. 3A) acting on crown i is given by

$$\vec{F}^{\,i}_{LJ}(\vec{r}^{\,ij}) = \begin{cases} -16\epsilon\left(4\frac{(\rho^i+\rho^j)^4}{|\vec{r}^{\,ij}|^5} - \frac{(\rho^i+\rho^j)^2}{|\vec{r}^{\,ij}|^3} - 3\frac{|\vec{r}^{\,ij}|}{(\rho^i+\rho^j)^2}\right)\hat{r}^{\,ij} & |\vec{r}^{\,ij}| < \rho^i + \rho^j \\ 0 & |\vec{r}^{\,ij}| \geq \rho^i + \rho^j \end{cases}, \tag{2}$$

where ϵ is a coefficient that scales the magnitude of the force, $\hat{r}^{\,ij}$ is the unit vector in the direction of $\vec{r}^{\,ij}$, and the $-3|\vec{r}^{\,ij}|/(\rho^i+\rho^j)^2$ term is introduced to shift the value of the force such that it approaches 0 when $|\vec{r}^{\,ij}| \to (\rho^i+\rho^j)^-$ and avoids the jump discontinuity that would otherwise occur at $|\vec{r}^{\,ij}| = \rho^i + \rho^j$.

We note that this is a modified Lennard-Jones force as it is described by a 4-2 potential rather than the considerably steeper 12-6 potential typically used in describing interatomic interactions [22]. We consider here only the repulsive regime of the potential, without the weak attraction that occurs at large separations. Futhermore, in practice, we fix $\vec{F}^{\,i}_{LJ}(\vec{r}^{\,ij}) = \vec{F}^{\,i}_{LJ}(0.5\vec{r}^{\,ij})$ for $|\vec{r}^{\,ij}| < 0.5(\rho^i + \rho^j)$ to prevent extremely large forces from occurring in the simulation.

The Lennard-Jones force $\vec{F}^{\,j}_{LJ}$ acting on crown j is of equal magnitude and points in the opposite direction along the unit vector $\hat{r}^{\,ji}$. For a system of multiple mutually shading crowns, the Lennard-Jones force $\vec{F}^{\,i}_{LJ}$ acting on crown i is the sum of all pairwise forces between crown i and all other crowns in the system.

Then, at each time step of the simulation, the change in position of crown i is given by the overdamped equation of motion

$$\vec{x}^{\,i}(t+\Delta t) = \vec{x}^{\,i}(t) + (\vec{F}^{\,i}_{sp} + \vec{F}^{\,i}_{LJ})\Delta t + \vec{\xi}, \tag{3}$$

where $\vec{\xi}$ is a random vector where each component is drawn from the normal distribution $\mathcal{N}(0, \sigma)$ with mean 0 and variance σ.

The radius of the crown increases according to the relation

$$r(t) = r_0 + \sqrt{\frac{At}{\pi}} \tag{4}$$

where A is the growth rate of the crown. For simplicity, in our simulations, we set the radius to be equal across each crown in the system.

To illustrate how self-organization can emerge from noise, we perform a parameter sweep over σ, the variance of the noise term $\vec{\xi}$ (Fig. 3C). The shaded area (represented as a fraction of the total area of the crowns) is highest for very low values of σ, decreases to a minimum for a moderate range of σ, and increases for high values of σ. With almost no noise, plants remain close to their initial linear configuration. Two overlapping crowns will experience repulsive forces parallel to the horizontal axis, but their neighbors to either side will produce anti-parallel repulsions in the opposite direction. With moderate noise, plants can laterally displace from the horizontal axis due to random fluctuations. This can result in "pioneer" plants that break the symmetry of the system to produce alternating off-axis deflections in a zig-zag pattern that minimize the shaded area. As noise increases further, random movements dominate over the repulsive forces, potentially leading to suboptimal disordered configurations with higher shaded area.

We simulate multiple-plant systems with our model using experimentally-determined parameters: 5 plants are initially separated by a distance of 11.5 cm and with an initial radius of 4.85 cm. The area of each crown increases linearly at a rate of 57 cm^2 (Fig. 2B) per day. Each timestep of the simulation represents one hour, and the variance in their random movements is set to 0.29 cm, the mean of the hourly step size distribution (Fig. 2D). Fig. 4A shows the initial configuration of the crowns, and the final self-organized configuration after 8 simulated days. We observe that the mean center-center distance between pairs of adjacent crowns agrees with experimental observations (Fig. 4B).

The spring constant k tunes how strongly crowns are tethered to their initial positions, while the coefficient ϵ of the Lennard-Jones force scales the strength of repulsion between shading crowns. In Fig. 4C, we explore the final center-center distance as a function of k and ϵ. We highlight a regime of the heatmap where the mean center-center distance matches that of the experimental values (approximately 14-16 cm).

For three pairs of k and ϵ within this regime ($k = 4, \epsilon = 8$, $k = 8, \epsilon = 14$, $k = 12, \epsilon = 20$), we run a sweep over values of the noise variance σ in the simulation (Fig. 4D). For each of these three pairs of parameters, the fractional shaded area as a function of σ shows a similar optimal trough as depicted in Fig. 3C. We observe that the experimentally-determined value of $\sigma = 0.29$ cm falls into the optimal noise range for the three parameter choices, indicating a robustness of the emergent self-organization to variations in the tethering and repulsive forces.

Discussion

Here we carried out experiments following the growth patterns of neighboring sunflowers closely grown in a row, reproducing self organization patterns reported by Pereira et al. [14]. In order to gain an understanding of the dynamics we developed a minimal model, describing the growing sunflower crowns as 2-D growing disks, tethered to their initial position, with the shade response represented by a repulsive interaction, and plant circumnutations interpreted as noise in the sunflower dynamics.

Informed by our experiments, we ran simulations while sweeping a number of parameters, such as the magnitude of the repulsive force and the magnitude of noise, resulting in a *phase space* of the total shaded area. A minimal shaded area corresponds to maximal photosynthesis, and is therefore critical for the survival of the collective.

These simulations revealed that, similarly to self-organization phenomena in motile systems, noise in growing systems also plays a crucial role, facilitating pattern formation. Furthermore, we found that the experimental value of noise associated with observed circumnutations generally corresponds to a minimal value of the total shaded area of the, maximizing photosynthesis. Our simulations also reveal that the measured noise is such that it is robust to variations in the repulsive interaction or the restoring force, which may correspond to, for example, variations in the shading due to leaf thickness, distance between leaves, or fluctuations in the environmental lighting.

While circumnutations are ubiquitous in plant systems, and generally associated with exploratory movements, a quantitative understanding of their role is elusive. Here we report, for the first time, their role in facilitating an optimal growth pattern for a group of interacting plants.

Conflict of Interest

The authors declare that they have no competing financial interests.

Funding

O.P. and Y.M. acknowledge support from the Human Frontiers Science Program (HFSP), Young Investigator Grant RGY0078/2019.

References

[1] S. Wolfram. Cellular automata as models of complexity. Nature, 311:419–424, 1984.

[2] F. Heylighen. The science of self-organization and adaptivity (eolss, paris). Nature, 5:pp 253–280, 1984.

[3] V. Bauchau. Emergence and reductionism: from the game of life to science of life. In B. Feltz, M. Crommelinck, and P. Goujon, editors, Self-Organization and Emergence in Life Sciences, page 29–40. (Springer, Dordrecht), 2006.

[4] K. N. Ganeshaiah and R. U. Shaanker. Frequency distribution of seed number per fruit in plants: A consequence of the self-organizing process? Curr Sci, 62:359–365, 1992.

[5] S. Kauffman. At Home in the Universe: The Search for the Laws of Self Organization and Complexity. Oxford Univ Press, Oxford, 1996.

[6] D. Sumpter, J. Buhl, D. Biro, and I. Couzin. Information transfer in moving animal groups. Theory in Biosciences, 127(2):177–186, 2008.

[7] H. Ling, G.E. Mclvor, J. Westley, K. van der Vaart, J Yin, R.T. Vaughan, A. Thornton, and N.T. Ouellette. Collective turns in jackdaw flocks: kinematics and information transfer. Journal of the Royal Society Interface, 16(159):20190450, 2019.

[8] M. Boos, J. Pritz, S. Lange, and M. Belz. Leadership in moving human groups. PLOS Computational Biology, 10(4):e1003541, 2014.

[9] B. Balázs, G. Vásárhelyi, and T. Vicsek. Adaptive leadership overcomes persistence-responsivity trade-off in flocking. Journal of the Royal Society Interface, 17(167):20190853, 2020.

[10] Dieu My T. Nguyen, Michael L. Iuzzolino, Aaron Mankel, Katarzyna Bozek, Greg J. Stephens, and Orit Peleg. Flow-mediated olfactory communication in honeybee swarms. Proceedings of the National Academy of Sciences, 118(13):e2011916118, 2021.

[11] O. Lejeune, M. Tlidi, and P. Couteron. Localized vegetation patches: A self-organized response to resource scarcity. Phys. Rev. E, 66:010901, Jul 2002.

[12] E. Sheffer, H. Yizhaq, E. Gilad, M. Shachak, and E. Meron. Why do plants in resource-deprived environments form rings? Ecological Complexity, 4(4):192–200, 2007.

[13] P. Couteron, F. Anthelme, M. Clerc, D. Escaff, C. Fernandez-Oto, and M. Tlidi. Plant clonal morphologies and spatial patterns as selforganized responses to resource limited environments. Philos Trans A Math Phys Eng Sci A, 372(140102), 2014.

[14] M. L. Pereira, V. O. Sadras, W. Batista, J. J. Casal, and A. J. Hall. Light-mediated self-organization of sunflower stands increases oil yield in the field. Proceedings of the National Academy of Sciences, 114:7975–7980, 2017.

[15] Jorge J Casal. Photoreceptor Signaling Networks in Plant Responses to Shade. Annual Review of Plant Biology, 64(1):403 – 427, 2013.

[16] C. L. Ballaré, A. L. Scopel, S. R. Radosevich, and R. E. Kendrick. Phytochrome-mediated phototropism in de-etiolated seedlings. Plant Physiol., 1007:170–7, 1992.

[17] G. A. Maddonni, M. E. Otegui, B. Andrieu, M. Chelle, and J. J. Casal. Maize leaves turn away from neighbors. Plant Physiol., 130:1181–89, 2002.

[18] A. Novoplansky, D. Cohen, and T. Sachs. How portulaca seedlings avoid their neighbours. Oecologia, 82:490–93, 1990.

[19] Renaud Bastien, Tomas Bohr, Bruno Moulia, and Stéphane Douady. Unifying model of shoot gravitropism reveals proprioception as a central feature of posture control in plants. Proceedings of the National Academy of Sciences, 110(2):755–760, 2013.

[20] Renaud Bastien, Stéphane Douady, and Bruno Moulia. A Unified Model of Shoot Tropism in Plants: Photo-, Gravi- and Propio-ception. PLOS Computational Biology, 11:e1004037, 2015.

[21] T. L. Hedrick. Software techniques for two- and three-dimensional kinematic measurements of biological and biomimetic systems. Bioinspiration & Biomimetics, 3(3):034001, 2008.

[22] J. E. Lennard-Jones. Cohesion. Proceedings of the Physical Society, 43(5):461–482, 1931.